PCCP

ROYAL SOCIETY OF CHEMISTRY

PAPER

View Article Online
View Journal | View Issue

Cite this: *Phys. Chem. Chem. Phys.*, 2022, **24**, 20941

A new ratiometric switch "two-way" detects hydrazine and hypochlorite *via* a "dye-release" mechanism with a PBMC bioimaging study†

Sangita Das, *[abc] Lakshman Patra,[a] Partha Pratim Das,[d] Kakali Ghoshal,[e] Saswati Gharami,[a] James W. Walton,[b] Maitree Bhattacharyya[e] and Tapan Kumar Mondal *[a]

A new ratiometric fluorescent probe (*E*)-2-(benzo[*d*]thiazol-2-yl)-3-(8-methoxyquinolin-2-yl)acrylonitrile (**HQCN**) was synthesised by the perfect blending of quinoline and a 2-benzothiazoleacetonitrile unit. In a mixed aqueous solution, **HQCN** reacts with hydrazine (N_2H_4) to give a new product 2-(hydrazonomethyl)-8-methoxyquinoline along with the liberation of the 2-benzothiazoleacetonitrile moiety. In contrast, the reaction of hypochlorite ions (OCl^-) with the probe gives 8-methoxyquinoline-2-carbaldehyde. In both cases, the chemodosimetric approaches of hydrazine and hypochlorite selectively occur at the olefinic carbon but give two different products with two different outputs, as observed from the fluorescence study exhibiting signals at 455 nm and 500 nm for hydrazine and hypochlorite, respectively. A UV-vis spectroscopy study also depicts a distinct change in the spectrum of **HQCN** in the presence of hydrazine and hypochlorite. The hydrazinolysis of **HQCN** exhibits a prominent chromogenic as well as ratiometric fluorescence change with a 165 nm left-shift in the fluorescence spectrum. Similarly, the probe in hand (**HQCN**) can selectively detect hypochlorite in a ratiometric manner with a shift of 120 nm, as observed from the fluorescence emission spectra. **HQCN** can detect hydrazine and OCl^- as low as 2.25×10^{-8} M and 3.46×10^{-8} M, respectively, as evaluated from the fluorescence experiments again. The excited state behaviour of the probe **HQCN** and the chemodosimetric products with hydrazine and hypochlorite are studied by the nanosecond time-resolved fluorescence technique. Computational studies (DFT and TDDFT) with the probe and the hydrazine and hypochlorite products were also performed. The observations made in the fluorescence imaging studies with human blood cells manifest that **HQCN** can be employed to monitor hydrazine and OCl^- in human peripheral blood mononuclear cells (PBMCs). It is indeed a rare case that the single probe **HQCN** is found to be successfully able to detect hydrazine and hypochlorite in PBMCs, with two different outputs.

Received 31st May 2022,
Accepted 10th August 2022

DOI: 10.1039/d2cp02482a

rsc.li/pccp

1. Introduction

Hydrazine is extensively used as the rocket propellant in space systems.[1] It is an extremely important chemical reagent mainly used in pharmaceuticals, pesticides, emulsifiers, dyes, and corrosion inhibitors in various chemical industries.[2,3] It is highly flammable and can be used for explosions.[4] On the other hand, hydrazine is regarded as a model industrial toxin, which adversely affects human and animal health by damaging the nervous system.[5] Hydrazine can readily be introduced in humans by oral, dermal, or inhalation routes of exposure.[6] Extensive investigations with laboratory animals strongly indicate that hydrazine is carcinogenic, which could cause lung, liver, and kidney cancers. The EPA (the U.S. Environmental Protection Agency) has marked hydrazine as an impending human carcinogen, whereas the World Health Organization (WHO) has suggested its threshold limit value (TLV) as 10 ppb.[7,8] Therefore, in real samples, the concentration of N_2H_4 must be controlled to lower than 10 ppb.

[a] *Department of Chemistry, Jadavpur University, Kolkata-700032, India. E-mail: tkmondal_ju@yahoo.com*
[b] *Department of Chemistry, Durham University, Durham, DH1 3LE, UK. E-mail: sangita.das@durham.ac.uk, sangitadas2327@gmail.com, sangita.das@kist-europe.de*
[c] *KIST Europe Forschungsgesellschaft mbH, Campus E71, 66123 Saarbrücken, Germany*
[d] *Center for Novel States of Complex Materials Research, Seoul National University, Seoul 08826, Republic of Korea*
[e] *Department of Biochemistry, University of Calcutta, Kolkata-700019, India*

† Electronic supplementary information (ESI) available. CCDC 1858041. For ESI and crystallographic data in CIF or other electronic format see DOI: https://doi.org/10.1039/d2cp02482a

On the contrary, reactive oxygen species (ROS) play crucial roles in many physiological processes in biological bodies.[9,10] Hypochlorous acid (HOCl) is known to be one of the most important biologically ROS-sub species. The endogenous production of hypochlorite is due to the peroxidation of chloride ions (mitochondrial electron transport chain) catalysed by the enzyme, namely myeloperoxidase (MPO).[11] However, the abnormal production of ROS is extremely harmful owing to variations in MPO levels. The excess concentration of OCl^- mainly involves unwanted oxidation of biomolecules.[12] Such oxidative stress can lead to a variety of diseases involving DNA mutations, aberrant electron transport, disruption of calcium homeostasis, activation of apoptosis, cardiovascular diseases, neuron degeneration, arthritis, and cancer.[13] Several studies have been reported so far by researchers based on the adverse impact of both hydrazine and hypochlorite towards flora and fauna,[14–33] albeit there is significant room for improvement.

Some relevant reports highlighting the probes detecting hydrazine and hypochlorite through different detection methods[34,35] are mentioned in this regard. Yu *et al.* fabricated an ICT-based probe to detect hydrazine,[36] but with a limitation of sensitivity in basic pH. The detection of hydrazine was hampered under basic conditions. In other two reports by Duan *et al.* and Wu *et al.*, a distinct naphthalimide-based ICT-mediated sensor was discussed, which exhibited a selective demasking of the acetate group using the chemodosimetric approach of hydrazine.[37,38] A few more studies also exist in the hydrazine sensor based on the chromatographic techniques,[39–41] mass spectrometry coupled with chromatography,[42] Raman spectroscopy[43] and capillary electrophoresis[44] *etc.* However, in most cases, these methods are time-consuming and require expensive instrumentation for implementation, which has some serious limitations for real-time monitoring.

On the other hand, the HOCl-sensitive fluorescent sensors follow different sensing mechanisms, for instance, the deoximation of fluorescent oximes,[45,46] chlorination of thioesters or amides,[47,48] and oxidations of thioethers to selenoxides.[49,50] However, none of the above-mentioned studies have been able to identify simultaneously two important toxic analytes, namely hydrazine and hypochlorite in human PBMCs using fluorescence imaging at two different outputs.

Therefore, the interest is still there to develop powerful ratiometric fluorescent switches for the dynamic tracking and detection of N_2H_4 and OCl^- in living systems with high sensitivity and good selectivity. Most importantly, a single sensor that can detect hydrazine and hypochlorite in PBMCs based on two different mechanisms with two different outputs is extremely rare.

Thus, in continuation of our previous work,[51–55] we have introduced a new switch (**HQCN**), which can detect the toxic N_2H_4 and OCl^- in the presence of other guest analytes with two different outputs. The synthesis, photophysical characteristics, and applications of this probe are manifested by highlighting several essential features in detail in the following 'Results and discussion' section, which consists of eleven subsections. In the 2.1. Section, entitled 'Synthesis of the probe', the fabrication of the probe has been discussed. Here, the 2-benzothiazoleacetonitrile moiety has been used as a new recognition site for the detection of N_2H_4 and OCl^- with two distinct outputs. The photophysical properties of **HQCN** in the presence of different guest analytes have been thoroughly examined and analysed based on the UV-vis and fluorescence studies in the next two Sections 2.2 and 2.3. Here, the mixed aqueous solution of HQCN (10 μM in CH_3OH–H_2O; 1/4, v/v) was prepared in the presence of a HEPES buffer (10 mM) solution at (pH = 7.2). In particular, the study to verify the specificity of the probe towards hydrazine and hypochloriteis indeed important and is emphasized in the next Section 2.4. entitled 'Selectivity study', which inevitably infers that the probe is an excellent fluorescence tool for the sensing of N_2H_4 and OCl^- at two different wavelength outputs without any interference. A comprehensive description of the sensing mechanisms can be found in Section 2.5. The aptness of the probe is indeed crucial and therefore is accomplished by studying the effect of pH and the kinetics of the probe on the target species, as demonstrated in Sections 2.6 and 2.7. These studies substantiate that **HQCN** is stable in the physiological system near the neutral pH for using it as a biomarker and successfully promoting the probe as a smart candidate for the prompt monitoring of hydrazine and hypochlorite. The lifetime of **HQCN** and its adducts (HQCN–N_2H_4 and HQCN–OCl) in the excited state were also studied using the nanosecond time-resolved fluorescence technique and was found to be in the order of nanoseconds (Section 2.8). As a support, the computational calculations (DFT and TDDFT) were performed, which validate the practical observation of the probe with N_2H_4 and OCl^- as mentioned in Section 2.9.

As far as the application of the probe is concerned, the bioimaging studies on **HQCN** were performed and are described in Section 2.10. The cell viability study explains that this fluorescent probe does not hamper any cellular damage while the bioimaging of human PBMCs by **HQCN** reflects it as an excellent tool to distinguish N_2H_4 and OCl^- at two different wavelength outputs.

However, the detailed synthetic procedure of the probe can be found in the 'Experimental' and the key findings are summarized in the 'Conclusion' section.

2. Results and discussion

2.1. Synthesis of the probe (HQCN)

The desired probe was synthesized as per Scheme 1. First, 8-methoxyquinoline-2-carbaldehyde and 2-benzothiazoleacetonitrile were prepared according to the procedures reported elsewhere by our group.[56,57]

As per Scheme 1, the condensation of 8-methoxyquinoline-2-carbaldehyde with 2-benzothiazoleacetonitrile in the presence of a catalytic amount of piperidine affords the probe (**HQCN**) as a yellow solid. Thereaftre, the probe was characterised *via* ^1H NMR, ^{13}C NMR, and HRMS, as shown in Fig. S20–S22 in the ESI.† In addition, the structure of the probe in the solid

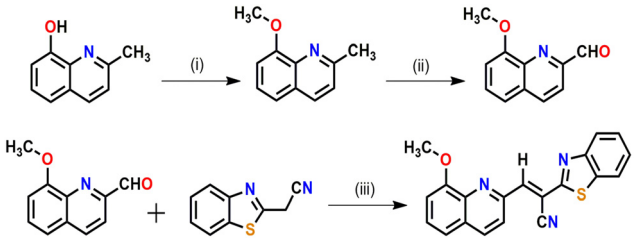

Scheme 1 Synthesis of the receptor (**HQCN**). *Reagents and conditions*: (i) CH_3I, K_2CO_3, and acetone, refluxed for 5 h. (ii) SeO_2 and 1,4-dioxane, refluxed for 4 h. (iii) Piperidine and EtOH, refluxed for 2 h.

state was confirmed by the single-crystal X-ray diffraction of the sample. The ORTEP plot with the atom numbering scheme is shown in Fig. S1 in the ESI.† The crystallographic data have been deposited at the Cambridge Crystallographic Data Center: Deposition numbers CCDC 1858041. A summary of the crystallographic data is provided in Table S1 in the ESI.†

2.2. UV-vis study

The developed sensor **HQCN** is supposed to show a notable UV-vis change upon the addition of hydrazine. In other words, the sensor was fabricated in such a way that only hydrazine could play a chemodosimetric mechanism among the other elements and leads to the prominent change. However, the preliminary optical characteristics were investigated by monitoring the UV-vis absorption study by taking the probe **HQCN** in a mixed aqueous methanol medium. It was observed that in the absence of any guest analytes the probe exhibited an absorbance maximum at 370 nm. The experiment was duly repeated several times and each time the strong absorbance peak appeared at 370 nm. This indicates that the probe in hand is highly stable under these physiological conditions. On the contrary, the addition of a trace amount of hydrazine causes a distinct change in the UV-vis profile. The absorption at 370 nm gradually decreased and a gradual increase in the absorption band at 272 nm was found at the same time (Fig. 1a).

In order to understand the mechanism more clearly and to make the probe more suitable for environmental and biological applications, an optimized mixed aqueous solution was prepared. The detail constituents of the solution prepared included a 10 μM probe in a mixture of CH_3OH and H_2O with a volume ratio of 1 : 4 in the presence of 10 mM HEPES buffer solution at a pH of 7.2. Thereafter, the selectivity of the probe was verified in the presence of several guest analytes such as hydroxylamine, ammonia, ethylenediamine, hydrazine, methylamine, *n*-butylamine, thiourea, and triethylamine. It is worth noting that the probe acted promptly only after the addition of hydrazine, whereas the other aforementioned amines remained almost mute to exhibit any significant change in the UV-vis spectroscopy (Fig. 1b). After the gradual addition of hydrazine from 0 to 5 equivalent, we found a characteristic change in the absorption spectra, where the peak at 370 nm rapidly decreased and a new peak appeared at 272 nm with a well-defined isosbestic point at 292 nm (Fig. 1). We consider that the change

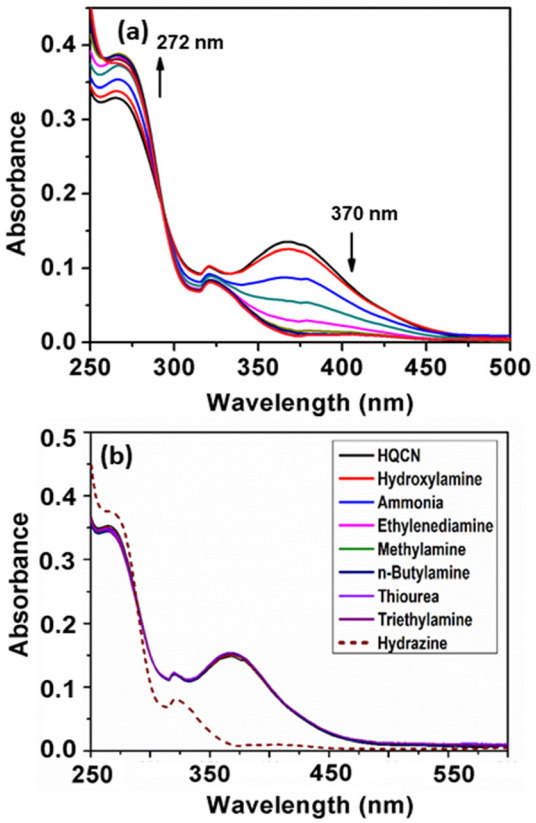

Fig. 1 (a) UV-vis spectra of **HQCN** (10 μM in CH_3OH–H_2O; 1/4, v/v in the presence of HEPES buffer (10 mM) solution at pH = 7.2) upon gradual addition of N_2H_4 (0 to 5 equivalents). Ratiometric spectra of **HQCN** were observed after the addition of N_2H_4. The absorption peak of **HQCN** at 370 nm gradually decreased and the peak at 272 nm gradually increased after the addition of N_2H_4 with an isosbestic point at 292 nm, (b) UV-vis spectra of **HQCN** (10 μM in CH_3OH–H_2O; 1/4, v/v in the presence of HEPES buffer (10 mM) solution at pH = 7.2) upon the addition of different guest analytes (addition of different guest amines from 0 to 5 equivalents). Apart from hydrazine, no significant change was observed for other amines.

in the absorbance profile after the addition of hydrazine may be attributed to the chemodosimetric approach of hydrazine to the olefinic carbon, which rearranges to provide the reaction-based product, 2-(hydrazonomethyl)-8-methoxyquinoline. The absorbance at 272 nm was plotted with the increase in the concentration of hydrazine in this regard, which clearly shows a good linear relationship in the range of 0–7.2 μM with the R^2 value of 0.99 (Fig. S6, ESI†).

The absorption phenomena of **HQCN** towards different ROS were investigated further following the same process as hydrazine, as described above. The constituents of the solution were also kept exactly the same during this study. The solution of **HQCN** in the mixed aqueous media showed strong absorbance at 370 nm. Interestingly, upon the addition of OCl^- to the colourless solution of **HQCN**, the peak at 370 nm decreased evidently and a low-energy absorption band centred at 512 nm started appearing (Fig. 2a). The isosbestic point was observed at 462 nm in this case. The change in the absorption behaviour here is attributed to the oxidation of the imine functionalized

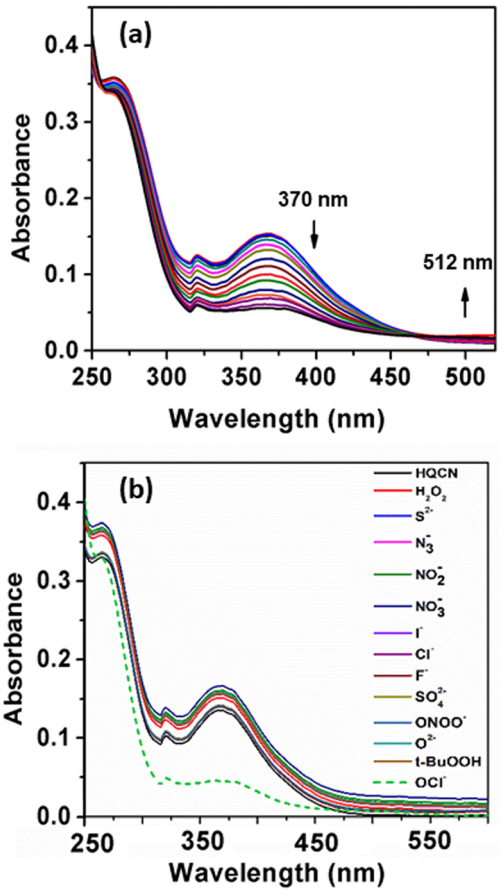

Fig. 2 (a) UV-vis spectra of **HQCN** (10 μM in CH_3OH–H_2O; 1/4, v/v in the presence of HEPES buffer (10 mM) solution at pH = 7.2) upon the gradual addition of OCl^- (0 to 5 equivalents). Ratiometric spectra of **HQCN** were observed after the addition of OCl^-. The absorption peak of **HQCN** at 370 nm gradually decreased and the peak at 512 nm gradually increased after the addition of OCl^- with an isosbestic point at 462 nm, (b) UV-vis spectra of **HQCN** (10 μM in CH_3OH–H_2O; 1/4, v/v in the presence of HEPES buffer (10 mM) solution at pH = 7.2) upon addition of different guest analytes (0 to 5 equivalents). Apart from OCl^-, no significant change was observed upon the addition of the other guest analytes.

to the corresponding aldehyde (HQA) system. It was again striking to observe that the other guest analytes of interest, namely H_2O_2, S^{2-}, N_3^-, NO_2^-, NO_3^-, I^-, Cl^-, F^-, SO_4^{2-}, $ONOO^-$, O^{2-} and *t*-BuOOH 10 μM, H_2O were not able to affect the UV-vis spectra of **HQCN** to a considerable extent (Fig. 2b). The change in the absorbance of **HQCN** at 512 nm in the UV-vis spectrum was plotted with the added OCl^- concentration and a good linear relationship was observed here as well with a good R^2 value of 0.99 (Fig. S7, ESI†).

2.3. Fluorescence study

In addition, we monitored the spectral behaviour of **HQCN** based on the fluorescence study. In this study, the spectroscopic evaluation of the probe was carried out at room temperature in a mixed aqueous methanol solution similar to the UV-vis absorption measurement (10 μM probe in CH_3OH/H_2O; 1/4, v/v in the presence of 10 mM HEPES buffer solution at pH, 7.2). Upon excitation at 370 nm, the probe in hand exhibited a strong emission peak with a maximum of 620 nm.

As per our expectation, no significant signal appeared at 455 nm, which evidences that the probe is stable in this mixed aqueous solution. However, based on the ICT (internal charge transfer) mechanism, significant changes in the fluorescence emission properties can occur in the presence of hydrazine in the mixed aqueous solution of HQCN. Therefore, the fluorescence spectra have been recorded systematically upon the addition of hydrazine and other amines in the mixed aqueous solution of HQCN at room temperature. After the interaction with hydrazine, the peak at 620 nm gradually decreased, whereas a concomitant new peak was observed at 455 nm with an increased intensity through a well-defined isoemissive point at 520 nm (Fig. 3a). In order to understand the chemodosimetric mechanism more clearly, we studied the reaction of

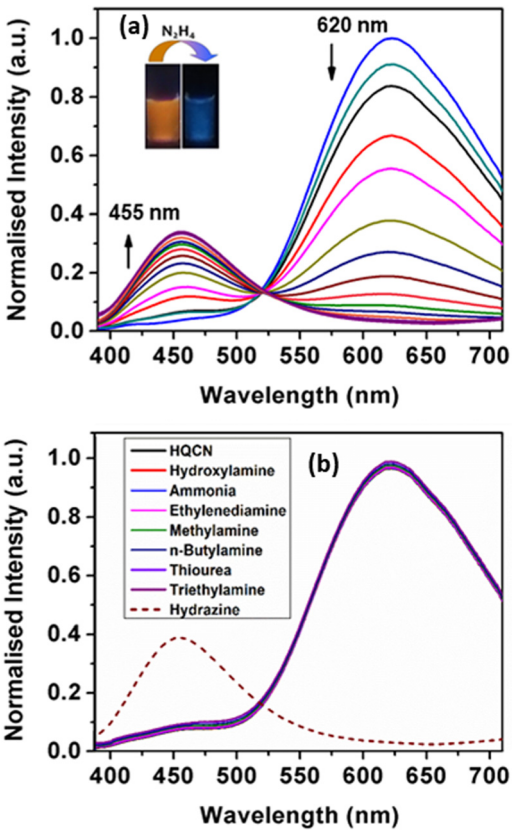

Fig. 3 (a) Fluorescence emission spectra of **HQCN** (10 μM in CH_3OH–H_2O; 1/4, v/v in the presence of HEPES buffer (10 mM) solution at pH = 7.2) upon the gradual addition of N_2H_4 (0 to 5 equivalents) where the λ excitation was 370 nm. Ratiometric spectra of HQCN were observed after the addition of N_2H_4. The emission peak of HQCN at 620 nm gradually decreased and the peak at 455 nm gradually increased after the addition of hydrazine with an isoemissive point at 520 nm, inset shows the visible emission of **HQCN** in the absence and presence of 2 equivalents of hydrazine upon irradiation under UV light, (b) Fluorescence emission spectra of **HQCN** (10 μM in CH_3OH–H_2O; 1/4, v/v in the presence of HEPES buffer (10 mM) solution at pH = 7.2) after the addition of different guest analytes (0 to 5 equivalents). Apart from hydrazine, no significant change was observed for other guest amines.

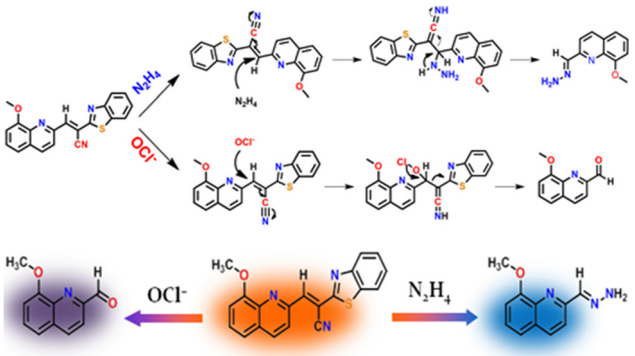

Scheme 2 Plausible mechanism for the recognition of N_2H_4 and OCl^- by HQCN. The probe in hand "two-way" detects hydrazine and hypochlorite *via* two different "dye-release" mechanisms.

hydrazine with the probe in hand by measuring the mass spectra.

A prominent peak observed in the MS spectrum at *m*/*z*, 202.1212 may represent the characteristics of the *in situ* product, *i.e.*, the HQCN–N_2H_4–adduct (Fig. S23, ESI†), which supports the proposed sensing mechanism. After the addition of hydrazine, an increase in the emission intensity at 455 nm was noticed, which was indeed associated with the hydrazinolysis at the olefinic carbon of **HQCN**. This further got conjugated at the nitrile portion and eventually liberated the recognition sight, *i.e.*, 2-benzothiazoleacetonitrile. This mechanism may contribute the ICT enhancement by forming the *in situ* adduct HQCN–N_2H_4, as depicted in Scheme 2.

The fluorogenic response of **HQCN** was studied as well by applying several other important amines. Analogous to the absorption phenomena, almost all the guest amines, including hydroxylamine, the well-known interfering compound with hydrazine, were found to be sufficiently non-responsive towards **HQCN** (Fig. 3b). Only hydrazine was able to make a distinct ratiometric change along with a significant left-shift of around 165 nm in the fluorescence spectra. This interesting feature was further confirmed when no significant changes in the emission spectrum of the receptor were observed upon performing the experiment in the presence of the excess amount of the guest amines. Therefore, the probe in this study is quite exclusive in detecting hydrazine among the other important amines. In this context, we have provided a table where the performance of our probe in hand is compared with other reported fluorescent sensors (comparison Table S4 in the ESI†). The ratio of the emission intensity of **HQCN** at 455 nm and 620 nm (I_{455}/I_{620}) was plotted with the added concentration of hydrazine. A good linear relationship was found here as well with the R^2 value of 0.99 (Fig. S4, ESI†). From the plot based on the emission spectra, the limit of detection limit (LOD) of hydrazine was evaluated thereafter following the equation, $DL = K \times (\mathrm{Sb1}/S)$, where '*K*' is considered as 3 and 'Sb1' and '*S*' define the standard deviation of the blank solution and the slope of the calibration curve, respectively.[58,59] The calculated detection limit was 2.25×10^{-8} M (Fig. S4, ESI†) which inevitably ensures that the **HQCN** has a very good efficiency to detect hydrazine.

In addition, the quantum yields of **HQCN** and HQCN–N_2H_4 adducts were calculated using the rhodamine-B (φ = 0.66 in ethanol) as a reference and those were 0.39 and 0.24, respectively.

During the observation of the fluorescence behavior of the compound **HQCN** in the presence of OCl^-, the constituents of the solution were kept the same as the previous experiments (10 μM probe in CH_3OH/H_2O; 1/4, v/v in the presence of 10 mM HEPES buffer solution at pH, 7.2). Here, the main emission band of **HQCN** at 620 nm was completely quenched upon the addition of OCl^-, whereas a new peak at 500 nm was found to originate, as observed in Fig. 4a. This was convincing evidence for the probe as the OCl^- sensor when we observed that the fluorescence intensity of **HQCN** remained almost unperturbed in the presence of the other guest analytes, namely, H_2O_2, S^{2-}, N_3^-, NO_2^-, NO_3^-, I^-, Cl^-, F^-, SO_4^{2-}, $OONO^-$, O^{2-} and *t*-BuOOH (Fig. 4b). The trend of the emission intensity was found to decrease upon increasing the concentration of OCl^-. We assign this phenomenon to the conversion of the imine group to the corresponding formyl group (aldehyde). A large shift of 120 nm was observed in this ratiometric spectrum. This large emission shift (ΔF = 120 nm) has been attributed to the accurate measurement of the intensities between the two emission peaks with a high ratiometric value. This chemodosimetric reaction of OCl^- to the imine functionality of **HQCN** eventually produced the oxidised product, *i.e.*, the HQCN–OCl^- adduct (8-methoxyquinoline-2-carbaldehyde). The formation of this *in situ* adduct was further confirmed by recording the mass spectra and ^{1}H NMR titration of **HQCN** after the addition of OCl^- (Fig. S24 and S25c, respectively, ESI†). The calculated quantum yield of the HQCN–OCl^- adduct was 0.45. The plot of the fluorescence intensity ratio at 500 and 620 nm (I_{500}/I_{620}) *versus* the added OCl^- concentration exhibited a good linear relationship with the R^2 value (Fig. S5, ESI†). The ratiometric probe exhibited a detection limit of 3.46×10^{-8} M for OCl^- (Fig. S5, ESI†). It was calculated from the fluorescence experimental data similarly as calculated for the hydrazine. Other potentially competing guest analytes did not hamper the recognition of the hypochlorite anions. Herein, HQCN acted as a fast-responding and highly sensitive sensor for the detection of OCl^-.

2.4. Selectivity study

Selectivity and sensitivity are the two very important constraints for assessing the performance of any chemodosimeters and chemosensors. In order to measure the selectivity, the experiment was performed with the probe in hand (**HQCN**) in the presence of the target species and the series of other guest analytes as mentioned above. Firstly, the specificity of the probe towards hydrazine was verified in addition to other important amines. To execute this experiment, the fluorescence intensities of the solutions of the **HQCN** and 2 equivalents of N_2H_4 at 455 nm were sequentially measured after the addition of different guest amines at much excess concentrations of ~3 equivalents (Fig. S2, ESI†). After observing the result, it was clear that the detection of hydrazine by **HQCN** was not at all hampered even in the presence of other interfering guest amines in excess amounts.

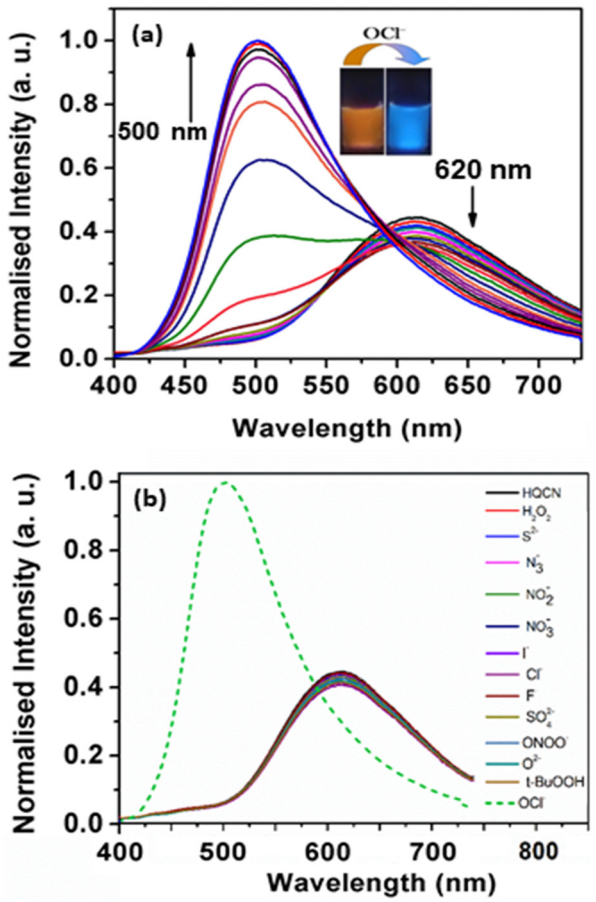

Fig. 4 (a) Fluorescence emission of **HQCN** (10 μM in CH_3OH–H_2O; 1/4, v/v in the presence of HEPES buffer (10 mM) solution at pH = 7.2) upon the gradual addition of OCl^- (0 to 5 equivalents). Ratiometric spectra of HQCN were observed after the addition of OCl^-, where the λ excitation was 370 nm. The fluorescence emission peak at 620 nm gradually decreased and the peak at 500 nm gradually increased after the addition of OCl^-. Inset shows the visible emission of **HQCN** in the absence and presence of 2 equivalents of HOCl upon irradiation under UV light. (b) Fluorescence emission spectra of **HQCN** (10 μM in CH_3OH–H_2O; 1/4, v/v in the presence of HEPES buffer (10 mM) solution at pH = 7.2) upon addition of different guest analytes (0 to 5 equivalents). Apart from OCl^-, no significant change was observed for other guest analytes.

Likewise, the sensitivity of **HQCN** towards OCl^- was studied as well by measuring the fluorescence output at 500 nm. The emission intensity of **HQCN** at 500 nm was measured in the same way after treatment with OCl^- (2 equivalents) in the presence of the other guest analytes (3.0 equivalents). In this case, also, it was quite evident that the recognition of OCl^- in the presence of other relevant analytes was not either hampered (Fig. S3, ESI†).

Therefore, we can firmly conclude that the probe in hand, **HQCN**, can be employed as a sensitive fluorescence tool for the detection of N_2H_4 and OCl^- at two different outputs with no significant interference.

2.5. Sensing mechanism of the probe

To obtain an insight into the proposed sensing process, we studied the reaction of **HQCN** with N_2H_4 and OCl^- based on mass spectrometry. When **HQCN** (20 μM) was treated with N_2H_4 (80 μM), a significant peak (Fig. S23, ESI†) was observed at m/z 202.1212, which is consistent with the value estimated with the reaction-based product, HQCN–N_2H_4–adduct (expected $[M + H]^+$ at 202.0980, Fig. S23, ESI†). The reaction mechanism is demonstrated in Scheme 2.

We have also analysed the reaction product HQCN–OCl^- (HQA) adduct (Fig. S24, ESI†). The chemodosimetric reaction-based product finally gave the corresponding aldehyde within a few seconds. This product was isolated for spectrochemical studies. The peak at 242.2538 m/z is consistent with the expected formylation product (expected $[M + H_2O + Cl^- + 2H^+]^+$ at 242.0589). The plausible chemodosimetric mechanism between **HQCN** and OCl^- is depicted in Scheme 2. **HQCN** was first oxidatively attacked by OCl^- to the imino group, which was further rearranged to form the formyl adduct (HQA).

2.6. Effect of pH

The effect of pH on the fluorescence response of **HQCN** towards N_2H_4 and OCl^- was also explored. The probe itself showed an insignificant change in the fluorescence intensity throughout the wide range of pH from 2.0 to 12. This strongly recommends that the **HQCN** is stable in the wide pH range and can be successfully applied in the biological samples. Thereafter, we recorded the changes in the fluorescence of **HQCN** after treatment with hydrazine. We found that under acidic pH the HQCN–N_2H_4 system exhibited no significant change in the fluorescence spectrum, more specifically the emission intensity at 455 nm (Fig. S8a, ESI†). On the contrary, at basic pH, above 8.3 in particular, a huge influence was observed towards the detection of hydrazine through a significant change in the emission intensity at 620 nm (Fig. S8b, ESI†). This experiment again supports the reliability of **HQCN** as an efficient fluorescence tool for the detection of hydrazine at biological pH.

Also, we have examined the pH sensitivity of the HQCN–OCl^- adduct (HQA). The HQA was quite sensitive towards the acidic pH (Fig. S9, ESI†) as an enhancement in the emission intensity at 620 nm was observed, especially above pH 6. Therefore, based on all these findings, we can unambiguously report the probe as a potential biomarker for biosamples.

2.7. Response rate

The reaction kinetics is a very important factor in terms of justifying the performance of any chemodosimeter. In this study, we calculated the rate constants of the two chemodosimetric reactions. In both cases, the fluorescence emission intensity of **HQCN** increased successively upon increasing the duration of the reaction with hydrazine and hypochlorite. Most importantly, the interaction of **HQCN** towards hydrazine and hypochlorite was found to be completed within a few seconds. The rate constants of the reactions between **HQCN** and hydrazine and between **HQCN** and hypochlorite were calculated in this regard. For that, firstly, the fluorescence spectra of **HQCN** were recorded after the addition of two equivalents of hydrazine. The fluorescence intensity at 455 nm was plotted with the reaction duration, which offered linearity up to around 50 seconds only, and afterward, no such increment was noticed

with the progression in the reaction time (Fig. S10, ESI†). Following the first-order rate equation, the rate constant (k), *i.e.*, the slope of the plot $\times$ 2.303 was calculated, which was 5.72×10^{-2} s^{-1}.

The kinetic study was conducted in the same way after the interaction of **HQCN** with OCl^-. A noteworthy increment in the emission intensity at 500 nm was observed and it reached the maxima at around 55 seconds (Fig. S11, ESI†). Based on the plot of the fluorescence intensity at 500 nm *versus* the duration of the reaction, the pseudo-first-order rate constant (k) was calculated. The calculated rate constant was found to be 8.33×10^{-2} s^{-1} for this reaction.

The considerably higher rate constants of the reactions demonstrate that our synthesized probe, **HQCN**, can also be effectively used as a real-time monitoring kit for hydrazine and hypochlorite at two different outputs.

2.8. Lifetime

We also examined the excited state behaviour of the probe **HQCN** and its reaction with hydrazine and hypochlorite based on the nanosecond time-resolved fluorescence technique, as shown in Fig. 5. In this study, the radiative rate constants were calculated according to the equation[60] $\tau^{-1} = k_r + k_{nr}$, where k_r, which can be related to the emission quantum yield and lifetime as Φ_f/τ defines the radiative rate constant, whereas k_{nr} defines the non-radiative rate constant of **HQCN** and the adducts, namely, HQCN–N_2H_4 and HQCN–OCl^- (HQA). The calculated rate constants are mentioned in Table S2 in the ESI.† The calculated τ was found to be 0.7 ns (χ^2 = 1.21) for **HQCN**, 6.32 ns (χ^2 = 1.15) for HQCN + N_2H_4 and 5.75 ns (χ^2 = 1.09) for HQCN + OCl^-.

2.9. Computational study

In this section, we report the relationship between the structural changes of **HQCN** and its complexes (with hydrazine and hypochlorite) and their optical responses. This theoretical calculation was evaluated by the density functional theory (DFT) and the time-dependent density functional theory (TDDFT) with the B3LYP/6-31+G(d) method in the Gaussian 09W, Revision D.01 program and visualized using the Gauss view program.[61,62] The optimized geometry and the highest occupied molecular orbital (HOMO) and lowest unoccupied molecular orbital (LUMO) of **HQCN** are depicted in Fig. S12, the ESI.† For TDDFT calculations, a solvent correction was incorporated using the CPCM model and methanol was chosen as the solvent. The calculated absorption spectra show peaks at 461.47 nm (f = 0.4150), 392.12 nm (f = 0.6966), and 373.11 nm (f = 0.0873) for **HQCN**, which are due to HOMO to LUMO, HOMO−1 to LUMO, HOMO−2 to LUMO transitions, respectively (ESI,† Table S3). However, for the reaction product (HQCN–N_2H_4), HOMO to LUMO+1 transition appeared at 277.93 nm (f = 0.9427), in the case of the other reaction-based product a strong transition appeared at 253.42 nm (f = 0.5423) corresponding to HOMO−2 to LUMO transition (Fig. S13–S15, ESI†).

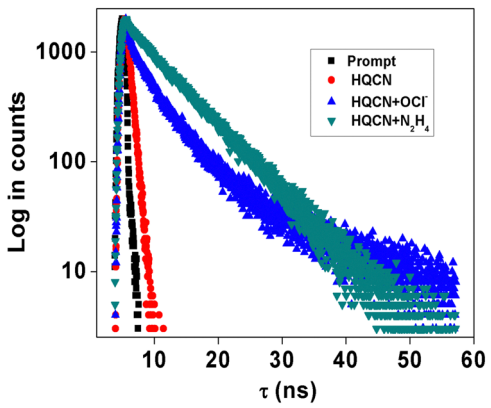

Fig. 5 Time-resolved fluorescence decay of HQCN (red), HQCN + OCl^- (blue), HQCN + N_2H_4 (green) and prompt (black) (λ excitation = 370 nm). The calculated τ was 0.7 ns (χ^2 = 1.21) for HQCN, 6.32 ns (χ^2 = 1.15) for HQCN + N_2H_4 and 5.75 ns (χ^2 = 1.09) for HQCN + OCl^-.

2.10. Bioimaging and MTT assay

HQCN is an excellent intracellular switch to detect hydrazine for its permeability as well as stability. Fig. 6(a) describes the bioimaging of human PBMCs by **HQCN** when there is no added N_2H_4 from outside. As shown in Fig. 6(b), very little or no blue fluorescence was observed. However, the addition of N_2H_4 significantly enhances the blue fluorescence (Fig. 6e) making it an excellent probe for bioimaging of (N_2H_4). In Fig. S16, ESI,† we can see that at the red channel, **HQCN**, shows a prominent intensity at the red channel (2759.3 $\pm$ 127.1) without hydrazine. The hydrazine untreated cells show almost insignificant fluorescence intensities at the blue channel (677.6 $\pm$ 27.5). However, after the addition of hydrazine, a significant increase ($P < 0.05$) in the blue fluorescence intensities was observed

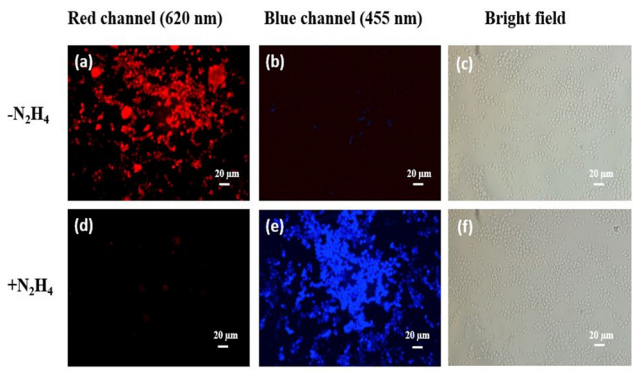

Fig. 6 Fluorescence images (40×) of human peripheral blood mononuclear cells (PBMCs) treated with 10 μM **HQCN** (a and b) and then the same was treated with 20 μM hydrazine solution (d and e), respectively. Images were taken in the red channel (620 nm) and blue channel (455 nm), (λ excitation = 370 nm). Larger cells are macrophages in PBMC populations, c and f are the corresponding bright-field images. The hydrazine untreated cells showed almost insignificant fluorescence intensities at the blue channel but showed a prominent color in the red channel, (a) However, after the addition of hydrazine, a significant increase in the blue fluorescence intensities was observed (e).

(3095 ± 125.7). Consequently, in this situation, the red fluorescence got expressively ($P < 0.05$) reduced (739 ± 40.8). The P values were evaluated using the one-way ANOVA followed by multiple comparisons for differences between groups (Fig. S16, ESI†).

Cell viability is represented in Fig. S17 (ESI†), where up to 50 μM concentration of **HQCN** show around 63.26% and 66.83% of viable cells with and without the presence of N_2H_4, respectively, predicting it to be a safe probe for use in a biological system. We have used 20 μmol l^{-1} **HQCN** solutions for imaging, which shows a fairly high number of viable cells (78.09%) in the presence of N_2H_4, concluding its non-toxic nature.

HQCN is an excellent probe for imaging biological samples for its permeability and stability. This fluorescent probe does not cause any cellular damage. Fig. 7, depicts the bioimaging of human PBMCs by **HQCN** in the absence and presence of OCl^-.

Therefore, the synthesis of a non-toxic fluorescent probe to detect HOCl is of extreme importance. In this study, in the absence of OCl^-, the shift from red fluorescence to green fluorescence is much less significant, but after the addition of OCl^-, a prominent increase in green fluorescence was observed. The mean fluorescence intensities were measured using ImageJ (Fig. S18, ESI†). The P values were calculated using one-way ANOVA followed by multiple comparisons for differences between the groups. The MTT assay (cell viability) is presented in Fig. S19 (ESI†), where increasing the concentrations of **HQCN** up to 50 μM showed the viable cells with and without OCl^- to be 53.73% and 56.18%, respectively.

2.11. Application as test-kit

Inspired by the superior sensitivity of **HQCN** towards hydrazine and hypochlorite, we further explored the probe for the detection of these species even in trace amounts. These experiments were mainly performed just to provide a qualitative idea of whether **HQCN** can be explored as a portable kit for sensing hydrazine and hypochlorite or not. To execute these experiments, a TLC plate was immersed in the 0.10 mM **HQCN** solution in CH_3OH and was dried in air.

After bubbling a large amount of contaminated air mixed with hydrazine, the **HQCN**-loaded TLC plate displayed prominent changes in colour. We recorded the fluorescence change with time by capturing the photographs of the particular TLC plate at different time intervals. After the exposure to the hydrazine vapour, the color of the TLC plate changed within 10 seconds, where it was monitored for up to 5 minutes.

However, a distinct change in the color of the plate can be observed in Fig. 8b–d. This promising result again recommends that the probe in hand **HQCN** can be employed as a highly sensitive candidate for the instant detection of the hydrazine and corroborates our previous inferences.

A similar experiment was conducted for the detection of OCl^-, as depicted in Fig. 9. The clearly distinguishable color change of the TLC plate also suggests that the probe offers a good portable assay kit for the hypochlorite sensor as well.

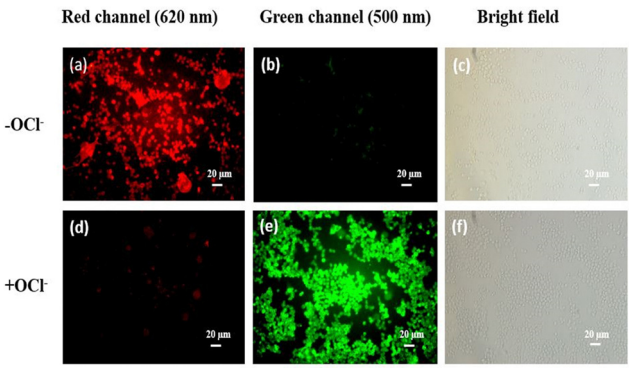

Fig. 7 Human PBMCs (40×) treated with 10 μmol l^{-1} **HQCN** under fluorescence emissions of 620 nm (a and d) and 500 nm (b and e), respectively. Images were captured before and after 50 minutes of incubation in dark. The cells showed almost insignificant fluorescence intensities at the green channel in the absence of OCl^- but showed a prominent color in the red channel (b and a, respectively). However, in the presence of OCl^-a significant increase in the green fluorescence intensity was observed (e). Bright field image of the cells (c) before and (f) after treatment.

3. Experimental

Synthesis of the probe (HQCN)

8-Methoxyquinoline-2-carbaldehyde (0.5 g, 2.67 mmol) and benzothiazole-2-yl-acetonitrile (0.47 g, 2.70 mmol) were added together in an ethanol (10 mL) solution and stirred at room temperature for 10 minutes. Piperidine (50 μL) and a catalytic amount of acetic acid were subsequently added to the reaction mixture and refluxed for 2 h under N_2-atm. The yellow-colored precipitate was formed after cooling the reaction mixture to room temperature, which was collected through filtration. The crude residue was purified by column chromatography using EtOAc/petroleum ether (1/4, v/v) as the eluent. Yield = 72%.

^{1}H NMR (300 MHz, $CDCl_3$): δ 4.16 (s, 3H), 7.13 (d, J = 6.9 Hz, 1H), 7.45 (t, J = 6.9 Hz, 2H), 7.55 (t, J =7.6 Hz, 2H), 7.93 (d, J = 7.3 Hz, 1H), 8.13 (d, J = 8.0 Hz, 1H), 8.34 (dd, $J1$ = 8.6 Hz, $J2$ = 8.6 Hz, 2H), 8.51 (s, 1H).

^{13}C NMR (75 MHz, $CDCl_3$): δ 56.56, 108.63, 110.10, 115.83, 119.46, 121.73, 123.47, 126.45, 126.99, 129.07, 129.50, 135.23, 137.11, 140.44, 146.76, 149.77, 153.65, 155.90, 162.55.

HRMS (ESI, positive): calcd for $C_{20}H_{13}N_3OS$ $[M + H]^+$ (m/z): 344.0858; found: 344.1226.

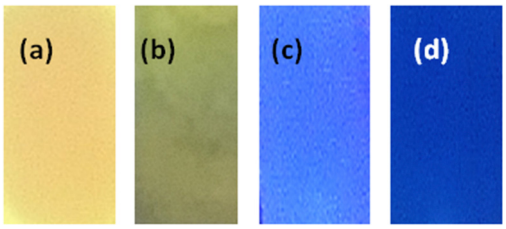

Fig. 8 Photographs of TLC plates, soaked in the solution of (a) HQCN and (b–d) after bubbling with hydrazine-contaminated air. Pictures taken after (b) 10 s (c) 60 s (d) 5 min.

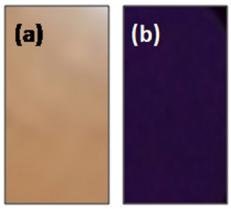

Fig. 9 Photographs of TLC plates, soaked in the solution of (a) HQCN and (b) after treating with OCl^- (pictures taken after 5 min).

4. Conclusions

In this study, a new ratiometric fluorescent switch **HQCN** has been introduced by the perfect combination of quinoline and a 2-benzothiazoleacetonitrile unit. The probe is highly selective and sensitive in detecting both the hydrazine and hypochlorite in a mixed aqueous solution following two different chemodosimetric mechanisms and consequently with two different emission outputs. The chemodosimetric hydrazinolysis of **HQCN** exhibited a ratiometric fluorescence change with a large left-shift of 165 nm and also could successfully detect hypochlorite in a ratiometric manner, exhibiting a left-shift of 120 nm in the fluorescence emission spectra, which unambiguously supported the diverse practical applications of the probe. Moreover, the quantitative low levels for the detection of hydrazine and hypochlorite were found to be 2.25×10^{-8} M and 3.46×10^{-8} M, respectively. These low LOD (limit of detection) values reflect the high performance of the probe. Some reports can be found in this regard, which claimed to act as either a hydrazine or hypochlorite sensor, although separately, while in most of the cases, the probes are not promising for the simultaneous detection of both hydrazine and OCl^-, as mentioned in Table S4 in the ESI.† Therefore, it is indeed exceptional that a probe can selectively detect the toxic hydrazine as well as hypochlorite based on two different mechanisms. Further, our probe in hand can be used as a real-time monitoring kit for the instant qualitative detection of N_2H_4 and OCl^- in samples in a facile way, namely by the dip-stick method, which is quite commendable when we consider the performance of the other probes reported so far for the on-site as well as real-time visual monitoring of the hydrazine and OCl^-. Although several important reports are available on the sensing of hydrazine and OCl^-, there is ample scope for further developing their potential. New probes with good water solubility, low cytotoxicity, excellent cell permeability from other molecular or ionic entities, and compatibility for live cell imaging are still in demand. The biological utility of the probe has also been established here based on the bioimaging studies, which confirm **HQCN** as a unique tool to distinguish hydrazine and hypochlorite for the first time in humans peripheral blood mononuclear cells at two different fluorescence outputs. A single sensor providing significant ratiometric changes in the physiological pH conditions during the sensing of both the hydrazine and hypochlorite in an environmental aqueous system is also quite rare. Therefore, our study could pave the way for developing new probes with dual sensing ability.

Conflicts of interest

There are no conflicts to declare.

Acknowledgements

Dr S. Das thanks the Science and Engineering Research Board (SERB), Govt. of India, for the National Post-Doctoral Fellowship (NPDF), File no. PDF/2016/001907 and Newton International Fellowships Royal Society (UK) for fellowship (ref: NIF\R1\182209). Prof. T. K. Mondal thanks CSIR, New Delhi, India for financial support (No. 01(2992)/19/EMR-II). S. Das Acknowledges Dr Krishnendu Aich, Department of Chemistry, Jadavpur University for helping in the excited state behaviour study of the compound.

Notes and references

1 S. D. Zelnick, D. R. Mattie and P. C. Stepaniak, Aviat., Occupational Exposure to Hydrazines: Treatment of Acute Central Nervous System Toxicity, *Space Environ. Med.*, 2003, **74**, 1285–1291.

2 S. S. Narayanan and F. Scholz, A comparative study of the electrocatalytic activities of some metal hexacyanoferrates for the oxidation of hydrazine, *Electroanalysis*, 1999, **11**, 465–469, DOI: **10.1002/(SICI)1521-4109(199906)11:7<465::AID-ELAN465>3.0.CO;2-%23**.

3 K. Yamada, K. Yasuda, N. Fujiwara, Z. Siroma, H. Tanaka, Y. Miyazaki and T. Kobayashi, Potential application of anion-exchange membrane for hydrazine fuel cell electrolyte, *Electrochem. Commun.*, 2003, **5**, 892–896, DOI: **10.1016/j.elecom.2003.08.015**.

4 U. Ragnarsson, Synthetic methodology for alkyl substituted hydrazines, *Chem. Soc. Rev.*, 2001, **30**, 205–213, DOI: **10.1039/B010091A**.

5 International Agency for Research on Cancer, *Re-evaluation of some organic chemicals, hydrazine, and hydrogen peroxide. IARC Monographs on the Evaluation of Carcinogenic Risk of Chemicals to Humans*, IARC, Lyon, 1999, vol. 71, pp. 991–1013, **https://monographs.iarc.fr/ENG/Monographs/vol71/mono71-43.pdf**.

6 Z. An, Z. Li, Y. He, B. Shi, L. Wei and M. Yu, Ratiometric luminescence detection of hydrazine with a carbon dots–hemicyanine nanohybrid system, *RSC Adv.*, 2017, **7**, 10875–10880, DOI: **10.1039/C6RA27844B**.

7 U.S. Environmental Protection Agency, *Integrated Risk Information System (IRIS) on Hydrazine/Hydrazine Sulfate, National Center for Environmental Assessment*, Office of Research and Development, Washington, DC, 1999.

8 A. Umar, M. M. Rahman, S. H. Kim and Y.-B. Hahn, Zinc oxide nanonail based chemical sensor for hydrazine detection, *Chem. Commun.*, 2008, 166–168, DOI: **10.1039/B711215G**.

9 X. Chen, X. Tian, I. Shin and J. Yoon, Fluorescent and luminescent probes for detection of reactive oxygen and

nitrogen species, *Chem. Soc. Rev.*, 2011, **40**, 4783–4804, DOI: 10.1039/C1CS15037E.

10 A. Gomes, E. Fernandes and J. L. F. C. Lima, Fluorescence probes used for detection of reactive oxygen species, *J. Biochem. Biophys. Methods*, 2005, **65**, 45–80, DOI: 10.1016/j.jbbm.2005.10.003.

11 N. Zhao, Y. H. Wu, R. M. Wang, L. X. Shi and Z. N. Chen, An iridium(III) complex of oximated 2,2′-bipyridine as a sensitive phosphorescent sensor for hypochlorite, *Analyst*, 2011, **136**, 2277–2282, DOI: 10.1039/C1AN15030H.

12 M. Whiteman, D. C. Hooper, G. S. Scott, H. Koprowski and B. Halliwell, Inhibition of hypochlorous acid-induced cellular toxicity by nitrite, *Proc. Natl. Acad. Sci. U. S. A.*, 2002, **99**, 12061–12066, DOI: 10.1073/pnas.152462399.

13 W. Y. Lin, L. L. Long, B. B. Chen and W. Tan, A Ratiometric Fluorescent Probe for Hypochlorite Based on a Deoximation Reaction, *Chem. – Eur. J.*, 2009, **15**, 2305–2309, DOI: 10.1002/chem.200802054.

14 G.-F. Wu, M.-X. Li, Y. Zhang, W.-G. Ji, Q.-B. Wang and Q.-X. Tong, *Mater. Electron. Eng.*, 2014, **1**, 3–5.

15 K. Li, H.-R. Xu, K.-K. Yu, J.-T. Hou and X.-Q. Yu, A coumarin-based chromogenic and ratiometric probe for hydrazine, *Anal. Methods*, 2013, **5**, 2653–2656, DOI: 10.1039/C3AY40148K.

16 Y. D. Lin and T. J. Chow, A pyridomethene–BF_2 complex-based chemosensor for detection of hydrazine, *RSC Adv.*, 2013, **3**, 17924–17929, DOI: 10.1039/C3RA42717J.

17 S. Goswami, S. Das, K. Aich, B. Pakhira, S. Panja, S. K. Mukherjee and S. Sarkar, A Chemodosimeter for the Ratiometric Detection of Hydrazine Based on Return of ESIPT and Its Application in Live-Cell Imaging, *Org. Lett.*, 2013, **15**, 5412–5415, DOI: 10.1021/ol4026759.

18 S. Goswami, K. Aich, S. Das, S. B. Roy, B. Pakhira and S. Sarkar, A reaction based colorimetric as well as fluorescence 'turn on' probe for the rapid detection of hydrazine, *RSC Adv.*, 2014, **4**, 14210–14214, DOI: 10.1039/C3RA46663A.

19 X.-Q. Zhan, J.-H. Yan, J.-H. Su, Y.-C. Wang, J. He, S.-Y. Wang, H. Zheng and J.-G. Xu, Thiospirolactone as a recognition site: Rhodamine B-based fluorescent probe for imaging hypochlorous acid generated in human neutrophil cells, *Sens. Actuators, B*, 2010, **150**, 774–780, DOI: 10.1016/j.snb.2010.07.057.

20 K. Dou, Q. Fu, G. Chen, F. Yu, Y. Liu, Z. Cao, G. L. Li, X. Zhao, L. Xia, L. X. Chen, H. Wang and J. M. You, A novel dual-ratiometric-response fluorescent probe for SO_2/ClO^- detection in cells and in vivo and its application in exploring the dichotomous role of SO_2 under the ClO^- induced oxidative stress, *Biomaterials*, 2017, **133**, 82–93, DOI: 10.1016/j.biomaterials.2017.04.024.

21 Q. Fu, G. Chen, Y. Liu, Z. Cao, X. Zhao, G. Li, F. Yu, L. Chen, H. Wang and J. You, In situ quantification and evaluation of ClO^-/H_2S homeostasis in inflammatory gastric tissue by applying a rationally designed dual-response fluorescence probe featuring a novel H^+-activated mechanism, *Analyst*, 2017, **142**, 1619–1627, DOI: 10.1039/C7AN00244K.

22 X. Jing, F. Yu and L. Chen, Visualization of nitroxyl (HNO) in vivo via a lysosome-targetable near-infrared fluorescent probe, *Chem. Commun.*, 2014, **50**, 14253–14256, DOI: 10.1039/C4CC07561G.

23 P. Liu, X. Jing, F. Yu, C. Lv and L. Chen, A near-infrared fluorescent probe for the selective detection of HNO in living cells and in vivo, *Analyst*, 2015, **140**, 4576–4583, DOI: 10.1039/C5AN00759C.

24 S. Goswami, S. Das, K. Aich, P. K. Nandi, K. Ghoshal, C. K. Quah, M. Bhattacharyya, H.-K. Fun and H. A. A.-Aziz, A rhodamine–quinoline based chemodosimeter capable of recognising endogenous OCl^- in human blood cells, *RSC Adv.*, 2014, **4**, 24881–24886, DOI: 10.1039/C4RA03200D.

25 S. Goswami, K. Aich, S. Das, B. Pakhira, K. Ghoshal, C. K. Quah, M. Bhattacharyya, H.-K. Fun and S. Sarkar, A Triphenyl Amine-Based Solvatofluorochromic Dye for the Selective and Ratiometric Sensing of OCl^- in Human Blood Cells, *Chem. – Asian J.*, 2015, **10**, 694–700, DOI: 10.1002/asia.201403234.

26 S. D. Hiremath, R. U. Gawas, D. Das, V. G. Naik, A. A. Bhosle, V. Priya Murali, K. Kumar Maiti, R. Acharya, M. Banerjee and A. Chatterjee, Phthalimide conjugation turns the AIE-active tetraphenylethylene unit non-emissive: its use in turn-on sensing of hydrazine in solution and the solid- and vapour-phase, *RSC Adv.*, 2021, **11**, 21269–21278, DOI: 10.1039/D1RA03563K.

27 S. Saha, S. Das, O. Sarkar, A. Chattopadhyay, K. Rissanen and P. Sahoo, Introduction of a luminescent sensor for tracking trace levels of hydrazine in insect pollinated cropland flowers, *New J. Chem.*, 2021, **45**, 17095–17100, DOI: 10.1039/D1NJ02661E.

28 C. Bao, S. Shao, H. Zhou and Y. Han, A new ESIPT-based fluorescent probe for the highly sensitive detection of amine vapors, *New J. Chem.*, 2021, **45**, 10735–10740, DOI: 10.1039/D1NJ01826D.

29 Y. Zhou, T. Liu, S. Zheng, X. Wang, M. Zhang, M. Irfan, Y. Zhang, H. Wang and Z. Zeng, A highly selective visual paper-based detector for hydrazine and MCL luminogens based on fluorinated-pyrrole-functionalized triphenylamine, *New J. Chem.*, 2021, **45**, 20173–20180 (*New J. Chem.*, 2021, 45, 20173–20180).

30 J. Pan, J. Ma, H. Liu, Y. Zhang and L. Lu, The preparation of a special fluorescent probe with an aggregation-induced emission effect for detecting hydrazine in water, *New J. Chem.*, 2021, **45**, 21151–21159, DOI: 10.1039/D1NJ03498G.

31 W. Zhang, W. Song and W. Lin, A novel ER-targeted two-photon fluorescent probe for monitoring abnormal concentrations of HClO in diabetic mice, *J. Mater. Chem. B*, 2021, **9**, 7381–7385, DOI: 10.1039/D1TB01327K.

32 K. Dąbrowa, M. Lindner, A. T. Gumkowska and J. Jurczak, Imino-thiolate-templated synthesis of a chloride-selective neutral macrocyclic host with a specific ''turn-off–on'' fluorescence response for hypochlorite (ClO^-), *Org. Chem. Front.*, 2021, **8**, 5258–5264, DOI: 10.1039/D1QO00504A.

33 K. Zhang, H. Wang, S. Cheng, C. Zhang, X. Zhai, X. Lin, H. Chen, R. Gao and W. Dong, A benzaldehyde–indole fused chromophore-based fluorescent probe for double-response to cyanide and hypochlorite in living cell, *Analyst*, 2021, **146**, 5658–5667, DOI: 10.1039/D1AN01015H.

34 A. Poghossian, M. Weil, A. G. Cherstvy and M. J. Schöning, Electrical monitoring of polyelectrolyte multilayer formation by means of capacitive field-effect devices, *Anal. Bioanal. Chem.*, 2013, **405**, 6425–6436, DOI: 10.1007/s00216-013-6951-9.

35 Maryam H. Abouzar, A. Poghossian, A. G. Cherstvy, A. M. Pedraza, S. Ingebrandt and M. J. Schöning, Label-free electrical detection of DNA by means of field-effect nanoplate capacitors: Experiments and modelling, *Phys. Status Solidi A*, 2012, **209**, 925–934, DOI: 10.1002/pssa.201100710.

36 K. Li, H.-R. Xu, K.-K. Yu, J.-T. Hou and X.-Q. Yu, A coumarin-based chromogenic and ratiometric probe for hydrazine, *Anal. Methods*, 2013, **5**, 2653–2656, DOI: 10.1039/C3AY40148K.

37 Y. Sun, D. Zhao, S. Fan and L. Duan, A 4-hydroxy-naphthalimide-derived ratiometric fluorescent probe for hydrazine and its in vivo applications, *Sens. Actuators, B*, 2015, **208**, 512–517, DOI: 10.1016/j.snb.2014.11.057.

38 X. Xia, F. Zeng, P. Zhang, J. Lyu, Y. Huang and S. Wu, An ICT-based ratiometric fluorescent probe for hydrazine detection and its application in living cells and in vivo, *Sens. Actuators, B*, 2016, **227**, 411–418, DOI: 10.1016/j.snb.2015.12.046.

39 H. Bhutani, S. Singh, S. Vir, K. K. Bhutani, R. Kumar, A. K. Chakraborti and K. C. Jindal, LC and LC-MS study of stress decomposition behaviour of isoniazid and establishment of validated stability-indicating assay method, *J. Pharm. Biomed. Anal.*, 2007, **43**, 1213–1220, DOI: 10.1016/j.jpba.2006.10.013.

40 M. Sun, L. Bai and D. Q. Lui, A generic approach for the determination of trace hydrazine in drug substances using in situ derivatization-headspace GC-MS, *J. Pharm. Biomed. Anal.*, 2009, **49**, 529–533, DOI: 10.1016/j.jpba.2008.11.009.

41 Y. Zhu, J. Zhang and S. Dong, Hydrazines probe of interaction of horseradish peroxidase with cryo-hydrogel, *Anal. Chim. Acta*, 1997, **353**, 45–52, DOI: 10.1016/S0003-2670(97)00385-1.

42 J.-A. Oh, J.-H. Park and H.-S. Shin, Sensitive determination of hydrazine in water by gas chromatography–mass spectrometry after derivatization with ortho-phthalaldehyde, *Anal. Chim. Acta*, 2013, **769**, 79–83, DOI: 10.1016/j.aca.2013.01.036.

43 X. Gu and J. P. Camden, Surface-Enhanced Raman Spectroscopy-Based Approach for Ultrasensitive and Selective Detection of Hydrazine, *Anal. Chem.*, 2015, **87**, 6460–6464, DOI: 10.1021/acs.analchem.5b01566.

44 J. Liu, W. Zhou, T. You, F. Li, E. Wang and S. Dong, Detection of Hydrazine, Methylhydrazine, and Isoniazid by Capillary Electrophoresis with a Palladium-Modified Microdisk Array Electrode, *Anal. Chem.*, 1996, **68**, 3350–3353, DOI: 10.1021/ac9604696.

45 X. Cheng, H. Jia, T. Long, J. Feng, J. Qin and Z. Li, A ''turn-on'' fluorescent probe for hypochlorous acid: convenient synthesis, good sensing performance, and a new design strategy by the removal of C[double bond, length as m-dash]N isomerization, *Chem. Commun.*, 2011, **47**, 11978–11980, DOI: 10.1039/C1CC15214A.

46 D. Li, Y. Feng, J. Lin, M. Chen, S. Wang, X. Wang, H. Sheng, Z. Shao, M. Zhu and X. Meng, A mitochondria-targeted two-photon fluorescent probe for highly selective and rapid detection of hypochlorite and its bio-imaging in living cells, *Sens. Actuators, B*, 2016, **222**, 483–491.

47 X. Chen, K.-A. Lee, X. Ren, J.-C. Ryu, G. Kim, J.-H. Ryu, W.-J. Lee and J. Yoon, Synthesis of a highly HOCl-selective fluorescent probe and its use for imaging HOCl in cells and organisms, *Nat. Protoc.*, 2016, **11**, 1219–1228, DOI: 10.1038/nprot.2016.062.

48 L. Cao, R. Zhang, W. Zhang, Z. Du, C. Liu, Z. Ye, B. Song and J. Yuan, A ruthenium(II) complex-based lysosome-targetable multisignal chemosensor for in vivo detection of hypochlorous acid, *Biomaterials*, 2015, **68**, 21–31, DOI: 10.1016/j.biomaterials.2015.07.052.

49 L. Yuan, L. Wang, B. K. Agrawalla, S.-J. Park, H. Zhu, B. Sivaraman, J. Peng, Q.-H. Xu and Y.-T. Chang, Development of Targetable Two-Photon Fluorescent Probes to Image Hypochlorous Acid in Mitochondria and Lysosome in Live Cell and Inflamed Mouse Model, *J. Am. Chem. Soc.*, 2015, **137**, 5930–5938.

50 L. Wu, I. C. Wu, C. C. DuFort, M. A. Carlson, X. Wu, L. Chen, C.-T. Kuo, Y. Qin, J. Yu, S. R. Hingorani and D. T. Chiu, Photostable Ratiometric Pdot Probe for in Vitro and in Vivo Imaging of Hypochlorous Acid, *J. Am. Chem. Soc.*, 2017, **139**, 6911–6918, DOI: 10.1021/jacs.7b01545.

51 S. Goswami, S. Das, K. Aich, D. Sarkar, T. K. Mondal, C. K. Quah and H. K. Fun, CHEF induced highly selective and sensitive turn-on fluorogenic and colorimetric sensor for Fe^{3+}, *Dalton Trans.*, 2013, **42**, 15113–15119, DOI: 10.1039/C3DT51974K.

52 S. Goswami, S. Das and K. Aich, An ICT based highly selective and sensitive sulfur-free sensor for naked eye as well as fluorogenic detection of Hg^{2+} in mixed aqueous media, *Tetrahedron Lett.*, 2013, **54**, 4620–4623, DOI: 10.1016/j.tetlet.2013.06.035.

53 S. Das, K. Aich, S. Goswami, C. K. Quah and H. K. Fun, FRET-based fluorescence ratiometric and colorimetric sensor to discriminate Fe^{3+} from Fe^{2+}, *New J. Chem.*, 2016, **40**, 6414–6420, DOI: 10.1039/C5NJ03598H.

54 S. Das, P. P. Das, J. W. Walton, K. Ghoshal, L. Patra and M. Bhattacharyya, FRET based ratiometric switch for selective sensing of Al^{3+} with bio-imaging in human peripheral blood mononuclear cells, *New J. Chem.*, 2021, **45**, 1853–1862, DOI: 10.1039/D0NJ05546H.

55 S. Das, P. P. Das, J. W. Walton, K. Ghoshal, L. Patra and M. Bhattacharyya, An excited state intramolecular proton transfer induced phosphate ion targeted ratiometric fluorescent switch to monitor phosphate ions in human peripheral blood mononuclear cells, *Dalton Trans.*, 2022, **51**, 10779–10786, DOI: 10.1039/D2DT00581F.

56 S. Das, K. Aich, L. Patra, K. Ghoshal, S. Gharami, M. Bhattacharyya and T. K. Mondal, Development of a

new fluorescence ratiometric switch for endogenous hypochlorite detection in monocytes of diabetic subjects by dye release method, *Tetrahedron Lett.*, 2018, **59**, 1130–1135, DOI: **10.1016/j.tetlet.2018.02.023**.

57 K. Wang, G. Lai, Z. Li, M. Liu, Y. Shen and C. Wang, A novel colorimetric and fluorescent probe for the highly selective and sensitive detection of palladium based on Pd(0) mediated reaction, *Tetrahedron*, 2015, **71**, 7874–7878, DOI: **10.1016/j.tet.2015.08.021**.

58 M. Shortreed, R. Kopelman, M. Kuhn and B. Hoyland, Fluorescent fiber-optic calcium sensor for physiological measurements, *Anal. Chem.*, 1996, **68**, 1414, DOI: **10.1021/ac950944k**.

59 W. Lin, L. Yuan, Z. Cao, Y. Feng and L. Long, A Sensitive and Selective Fluorescent Thiol Probe in Water Based on the Conjugate 1,4-Addition of Thiols to α,β-Unsaturated Ketones, *Chem. – Eur. J.*, 2009, **15**, 5096, DOI: **10.1002/chem.200802751**.

60 B. Valeur, *Molecular Fluorescence. Principles and Applications*, Wiley-VCH, Weinheim, Germany, 2002.

61 A. D. Becke, Density–functional thermochemistry. III. The role of exact exchange, *J. Chem. Phys.*, 1993, **98**, 5648–5652, DOI: **10.1063/1.464913**.

62 D. Andrae, U. Haeussermann, M. Dolg, H. Stoll and H. Preuss, Energy-adjusted ab initio pseudopotentials for the second and third row transition elements, *Theor. Chim. Acta*, 1990, **77**, 123–141, DOI: **10.1007/BF01114537**.

